PNAS
www.pnas.org

Supplementary Information for

Wildfires and climate change push low-elevation forests across a critical climate threshold for tree regeneration

KT Davis, SZ Dobrowski, PE Higuera, ZA Holden, TT Veblen, MT Rother, SA Parks, A Sala, and MP Maneta

Corresponding author: KT Davis
Email: Kimberley.Davis@umontana.edu

This PDF file includes:

Supplemental methods
Supplemental results
Figs. S1 to S22
Tables S1 to S5
References for SI reference citations

www.pnas.org/cgi/doi/10.1073/pnas.1815107116

Supplemental methods

Site selection

Within each fire in the NR, SW, and CA, sampling areas were selected based on the following criteria: (1) sites burned at moderate to high severity based on the Monitoring Trends in Burn Severity (MTBS) dataset, (2) sites were within 1 km of a road, (3) sites had *P. ponderosa* and/or *P. menziesii* according to "Existing Vegetation" layers (from CALVEG for CA; from the US Forest Service for all other regions), and (4) sites had either northerly (315-45°) or southerly (135-225°) aspects. We excluded areas that had post-fire management based on the FACTS database, geospatial data from individual forests, field observations, and conversations with local silviculturalists. Using a GIS, two to 12 sampling points were randomly placed within these sampling areas (depending on sampling area size). Because we were targeting sites with regeneration, sampling points that were farther than 100 m from a live seed source were excluded. The goal was to sample at least two sites per fire, but in the cases of some large fires, up to eight sites were sampled. In a few fires in the NR, only one site per fire was sampled. Selection of fires and sites from CO are described in more detail by Rother & Veblen (ref. 1) but generally followed a similar sampling scheme. A total of 19 sites in CA, 10 in CO, 40 in NR, and 21 in SW were sampled (Table S1 & S2). The SW sites receive on average 54% of their annual precipitation between July and September, while this value declines to 32% for the CO sites, 13% for the NR sites and 3% for the CA sites.

Bioclimatic data

Bioclimatic variables were calculated from gridded climate data from 1979-2015 with a resolution of 250 m at daily or sub-daily timescales (ref. 2), and then summarized to seasonal or annual values. To calculate mean summer VPD (June-August), daily minimum and maximum temperature and relative humidity, and daily net shortwave radiation were extracted from gridded datasets. Daily maximum VPD was calculated from the daily maximum temperature and daily minimum RH. The daily maximum saturation vapor pressure (e_s) was first calculated from the maximum temperature. Daily maximum actual vapor pressure (e_a) was then estimated using maximum temperature and minimum relative humidity. The VPD was then calculated as e_s minus e_a. Soil moisture and maximum land surface temperature (LST) were modeled using the ECH_20 ecohydrology model (ref. 3) following methods described by Simeone et al. (ref. 4). Simulations were run at a 3-hr time step from 1979-2015 assuming sparse canopy cover (5%) and leaf area index (0.1). Soil moisture was modeled in the upper 10 cm of the soil profile using gridded maps of soil properties. Sub-daily soil moisture and maximum LST outputs were then summarized to produce daily maximum LST and daily mean soil moisture. Soil moisture at 0-10 cm, the depths reached by young conifer seedling roots, was summarized to mean soil moisture of the driest month of the growing season (March to October) and mean spring soil moisture (March to May). The maximum LST observed during each year was retrieved for each site. Climatic water balance deficit was calculated at a daily time step following methods described by Hoylman et al. (ref. 5) and then summed for each year.

Boosted regression tree (BRT) models

Binomial BRT models were fit to data from each species separately, using a region-specific threshold of annual juvenile recruitment rates (# juveniles ha^{-1} yr^{-1}) to convert annual regeneration rates to a binary response (Table S1). To test the sensitivity of our results to these thresholds, we additionally conducted our analysis using a 50^{th} percentile threshold and juvenile presence/absence alone. In both cases we obtained similar results to the 25^{th} percentile thresholds described in the manuscript (Figs. S3-S7).

For BRT models we set the bag fraction to 0.75 and tree complexity to three. We started with a learning rate of 0.005 and reduced it incrementally until the models produced at least 1000 trees (final learning rate was 0.002 for ponderosa pine model and 0.001 for Douglas-fir model). We tested predictive performance by leaving out each site, fitting a BRT model with the same settings as above, predicting the holdout site, and then calculating accuracy (defined as the proportion of years with correct prediction) and the AUC statistic. When calculating accuracy, the threshold for determining success or failure of recruitment from the modeled probabilities was the value that maximized specificity and sensitivity for each site (Youden's J statistic; ref. 6).

In addition to results presented in the manuscript, we also used the models to hindcast annual recruitment probability at each site based on the site-specific annual climate time series (1981-2015; Fig. S8) while varying time-since-fire from 1 to 10 years. Distance to seed source (50 m) and fire severity (412, the median across all sites) were held constant. We then calculated the cumulative recruitment probability over years 1-5 and 1-10 following a hypothetical fire in each year from 1980 to 2010 (for cumulative recruitment probabilities for post-fire years 1-5) or 1980 to 2005 (for cumulative recruitment probabilities for post-fire years 1-10). We averaged these cumulative recruitment probabilities for sites within each region.

Temporal variability in observed tree recruitment rates

To quantify temporal variability in observed annual tree recruitment rates at each site and assess potential causes, we constructed age structures for each species-site combination (Figs. S14-S22). At each site, we calculated Pielou's evenness metric, which varied between 0.20 and 0.91, and indicates episodic (low values) or continuous (high values) recruitment (Fig. S13). We then modeled evenness as a linear function of tree species, shrub cover, 30-year mean (1980-2009) climatic water deficit (ref. 7), fire severity (dNBR), and all possible two-way interactions of these variables. Predictors and interactions that were not significant ($P > 0.05$) were not retained in the final model. Shrub cover data were not collected in CO and thus CO sites were excluded from this analysis. The total sample size for this analysis was 72 sites.

Supplemental results

BRT models

The BRT models performed well when cross validation by site was performed, with mean accuracies of 0.72 and 0.77, and AUC values of 0.79 and 0.83 for the ponderosa pine and Douglas-fir models, respectively. The AUC values for both species were significantly higher than 0.50 ($P < 0.001$; ref. 8). Accuracy and AUC were not biased by region (Fig. S2; Table S4).

Age structures

Figs. S14-S22 display all age structures from this study that had regeneration. Sites that are not shown, because they had no regeneration are as follows: In CA: ANT1N, ANT1S_ADJ, ANT2S, JKA1N, JKA3S_ADJ, MLT4N, MLT4S, RAL2S; in NR: BIC1, CFY1N, CFY1S, CFY2S, EAR1, EZN12S, EZN1S, EZN2S, FH2S; in SW: PEP2BN, PEP2S_ADJ, PEP3S, PEP5N, PEP5S, SED2S, SED3N, SED3S, SED6S, UN6N, UN7N. See Table S2 for site descriptions.

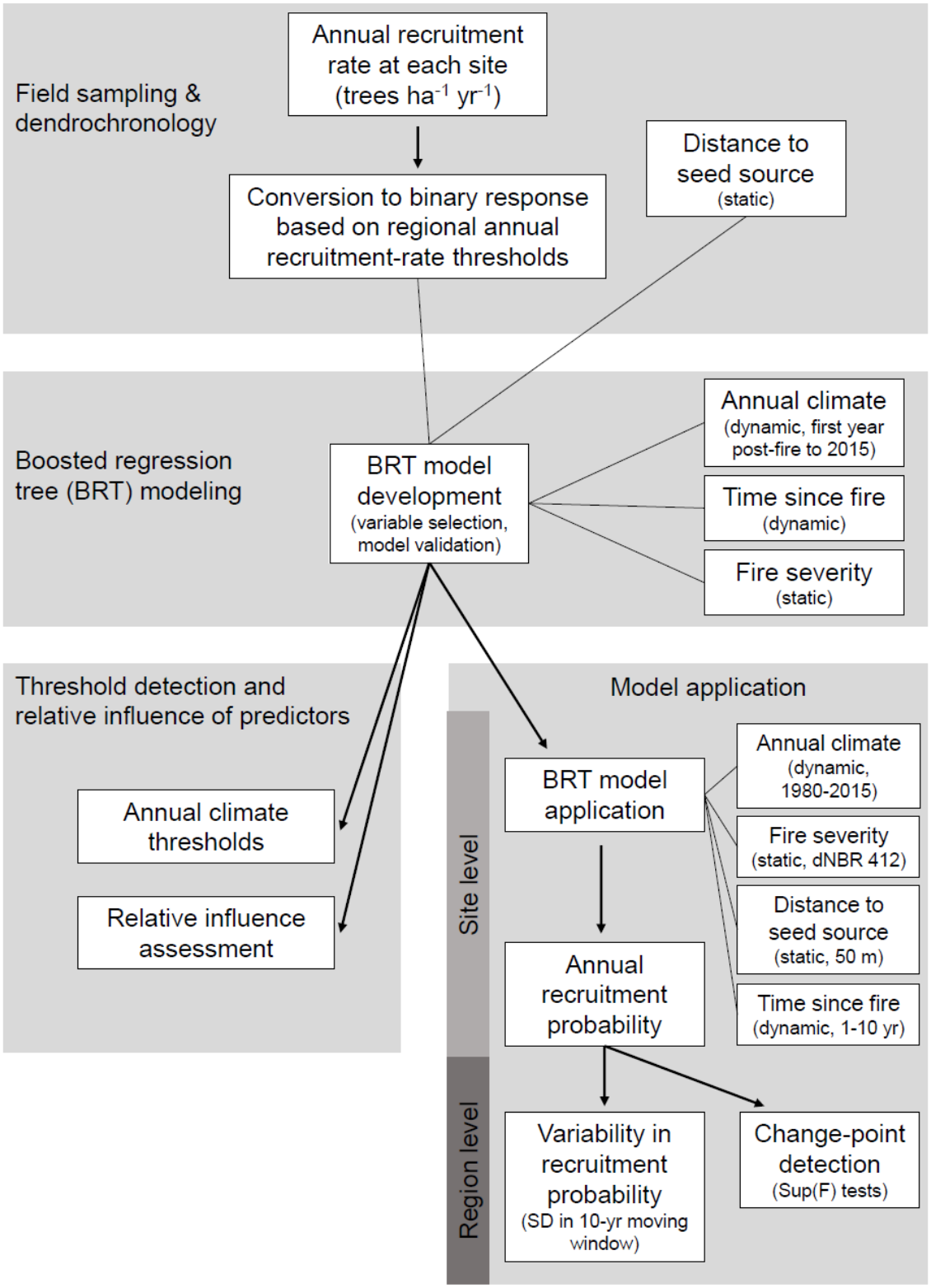

Figure S1. Flow diagram of methods. Boxes connected by lines indicate data input into models, while arrows indicate next steps in the analysis.

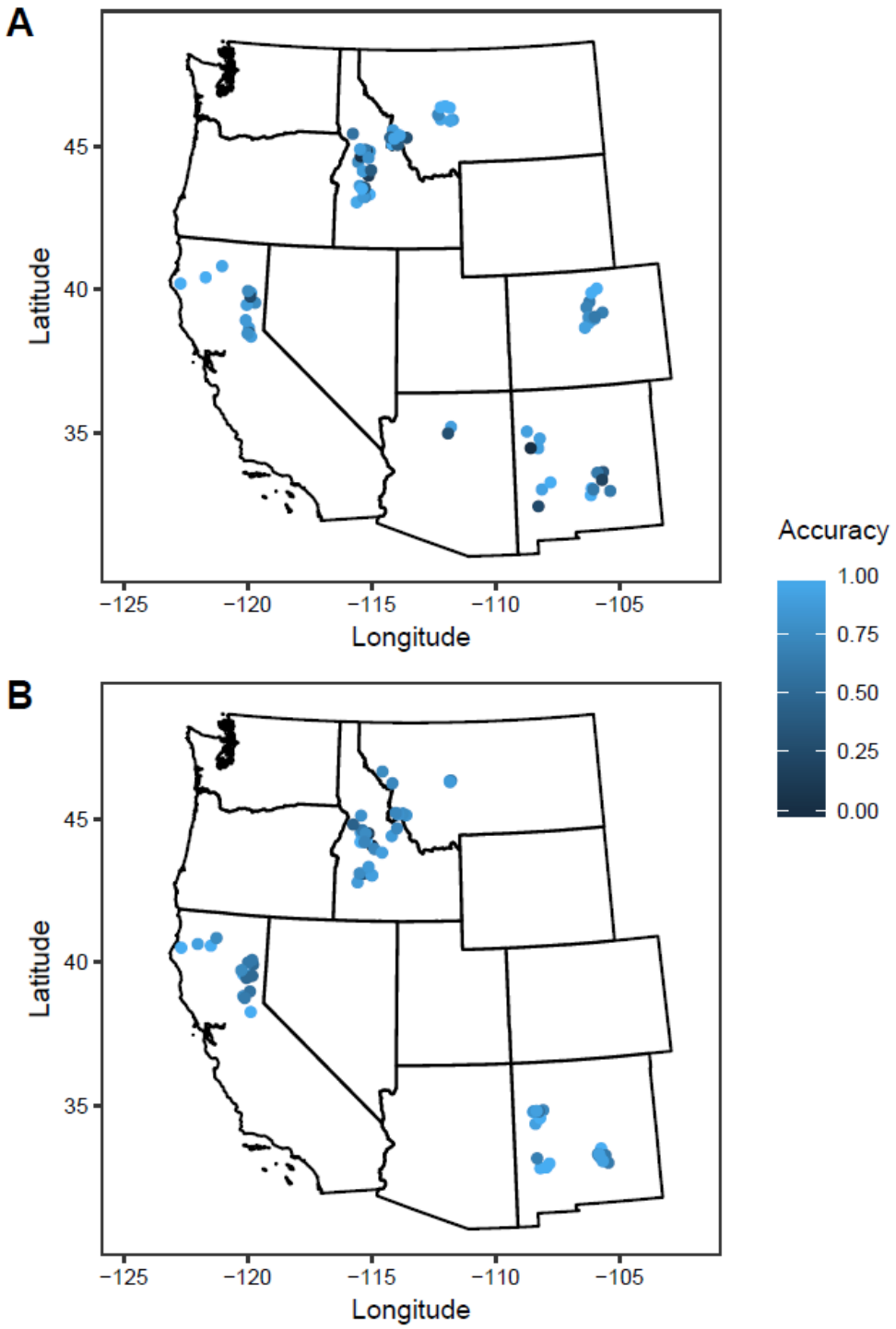

Figure S2. Map displaying the accuracy of predictions to each ponderosa pine (A) and Douglas-fir (B) site made from the ponderosa pine and Douglas-fir models fitted while leaving out that site. When calculating accuracy, the threshold for determining success or failure of recruitment from the modeled probabilities was the value that maximized specificity and sensitivity for each site (Youden's J statistic; ref. 6). Point locations are jittered for clarity.

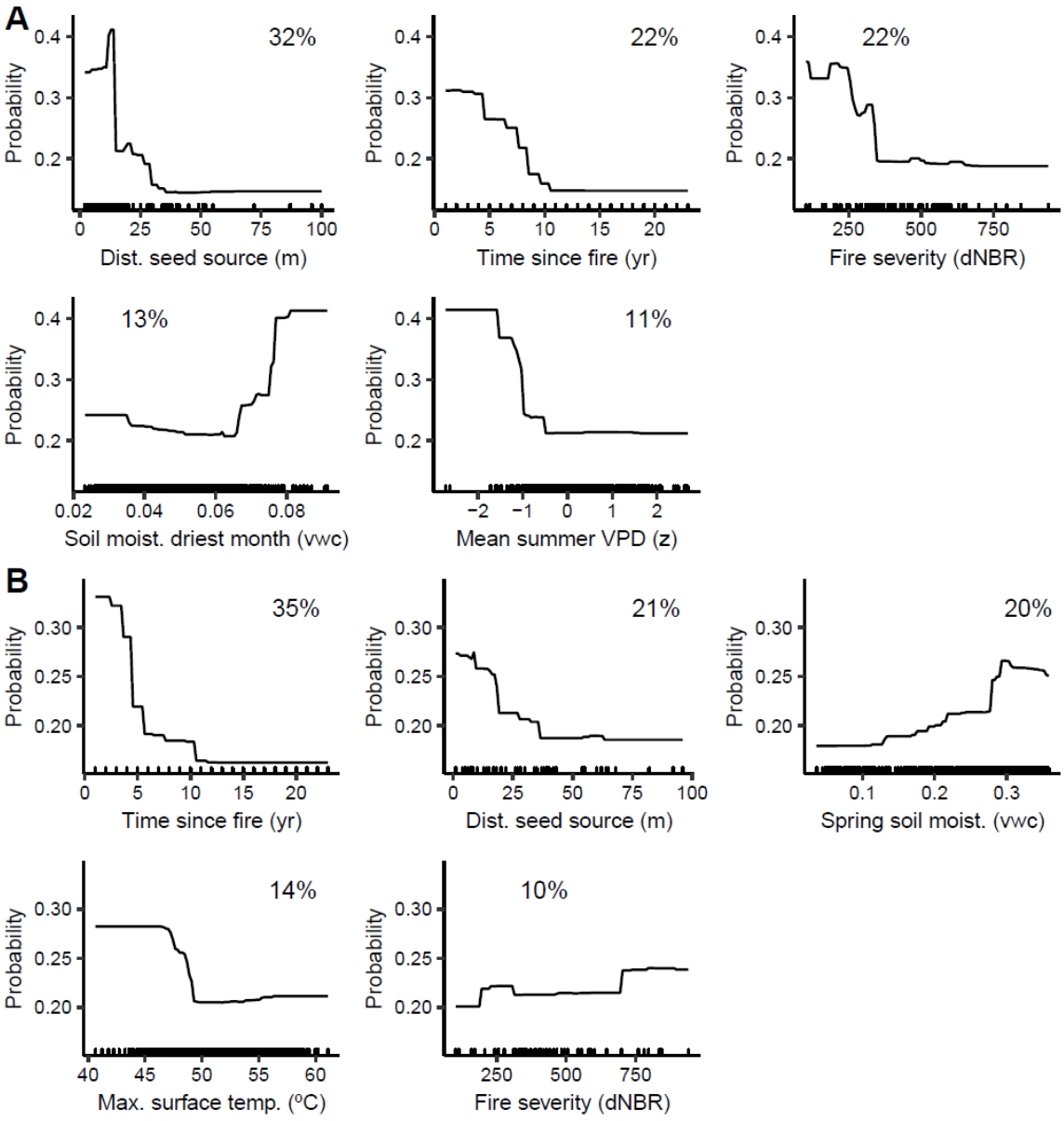

Figure S3. Partial dependency plots from final ponderosa pine (A) and Douglas-fir (B) boosted regression tree models showing the marginal effect of each variable on probability of crossing the recruitment threshold after accounting for the average effects of all other variables in the model. Percent values (%) on plots display the relative influence of that predictor. Vertical lines on x-axis (rug plot) show the distribution of observations in the dataset. The recruitment threshold in these models was the 25th percentile of recruitment density for years with recruitment for a given species in a given region (Table S1).

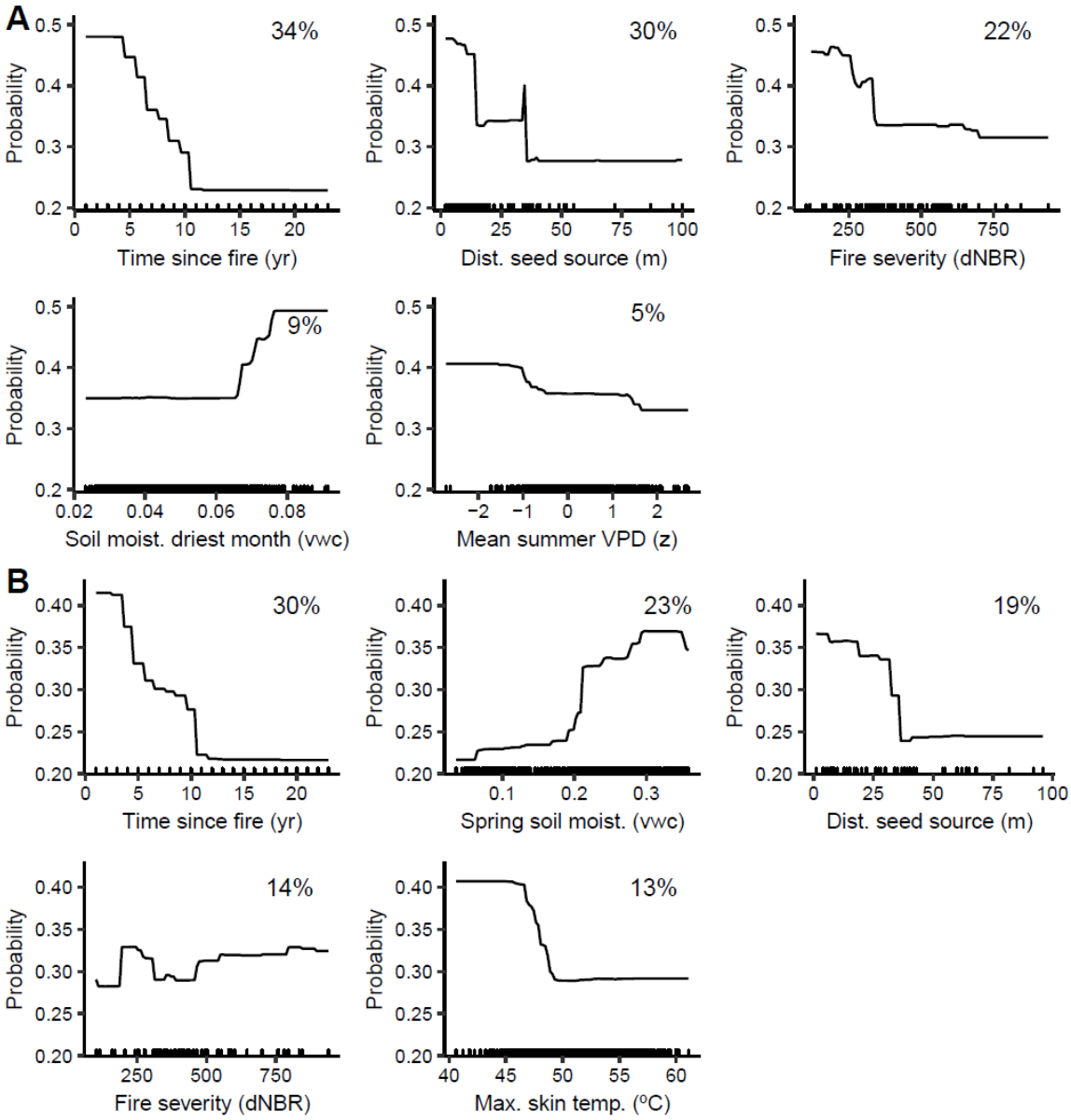

Figure S4. Partial dependency plots from final ponderosa pine (A) and Douglas-fir (B) boosted regression tree models showing the marginal effect of each variable on probability of presence of recruitment after accounting for the average effects of all other variables in the model. Percent values (%) on plots display the relative influence of that predictor. Vertical lines on x-axis (rug plot) show the distribution of observations in the dataset. The recruitment threshold in these models was 4 trees/ha (lowest density recorded in any plot in any year) which is equivalent to modeling the presence or absence of at least one seedling in a plot in each year (due to variable plot width).

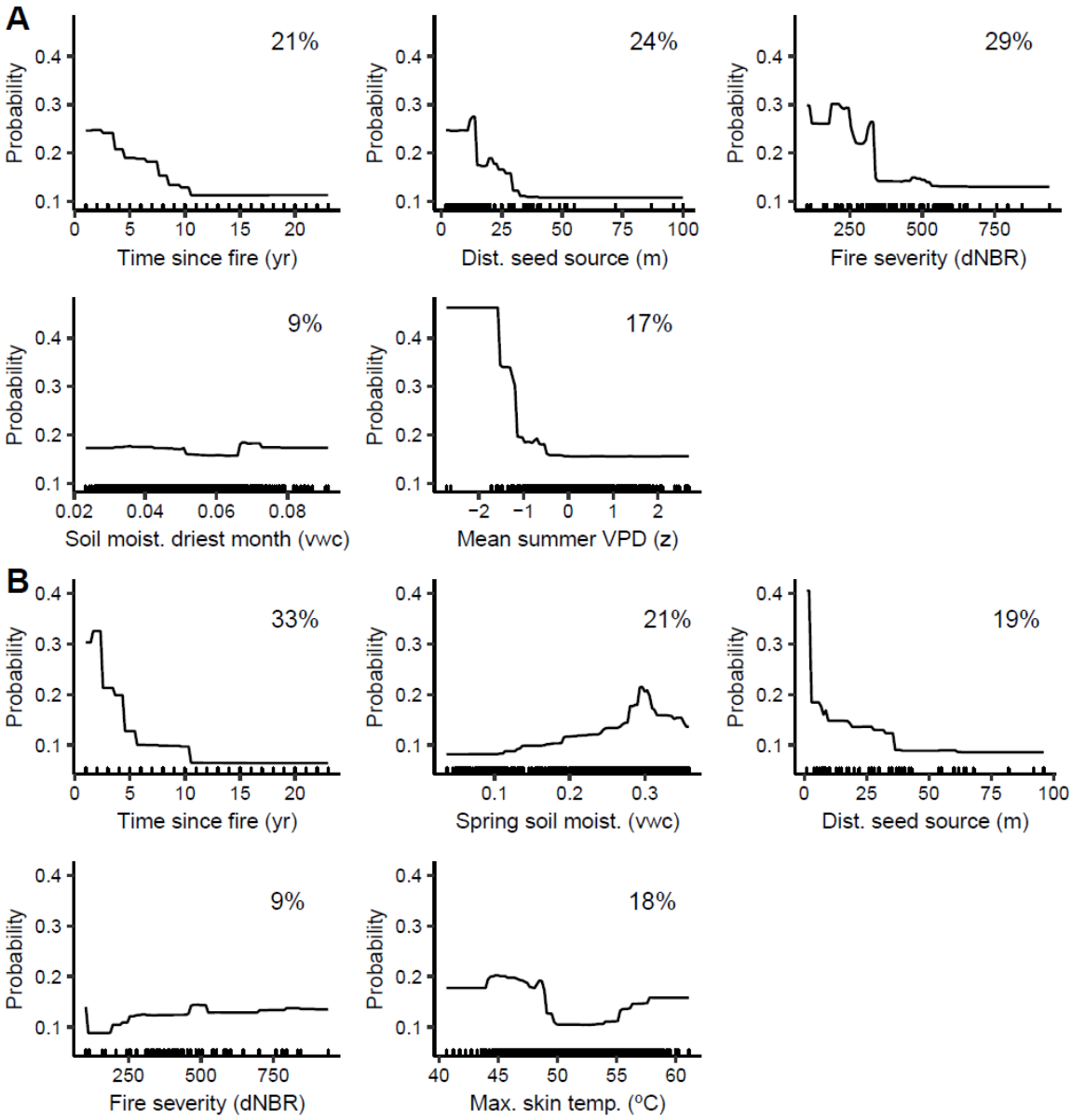

Figure S5. Partial dependency plots from final ponderosa pine (A) and Douglas-fir (B) boosted regression tree models showing the marginal effect of each variable on probability of crossing the recruitment threshold after accounting for the average effects of all other variables in the model. Percent values (%) on plots display the relative influence of that predictor. Vertical lines on x-axis (rug plot) show the distribution of observations in the dataset. The recruitment threshold in these models was the 50th percentile of recruitment density for years with recruitment for a given species in a given region (Table S1).

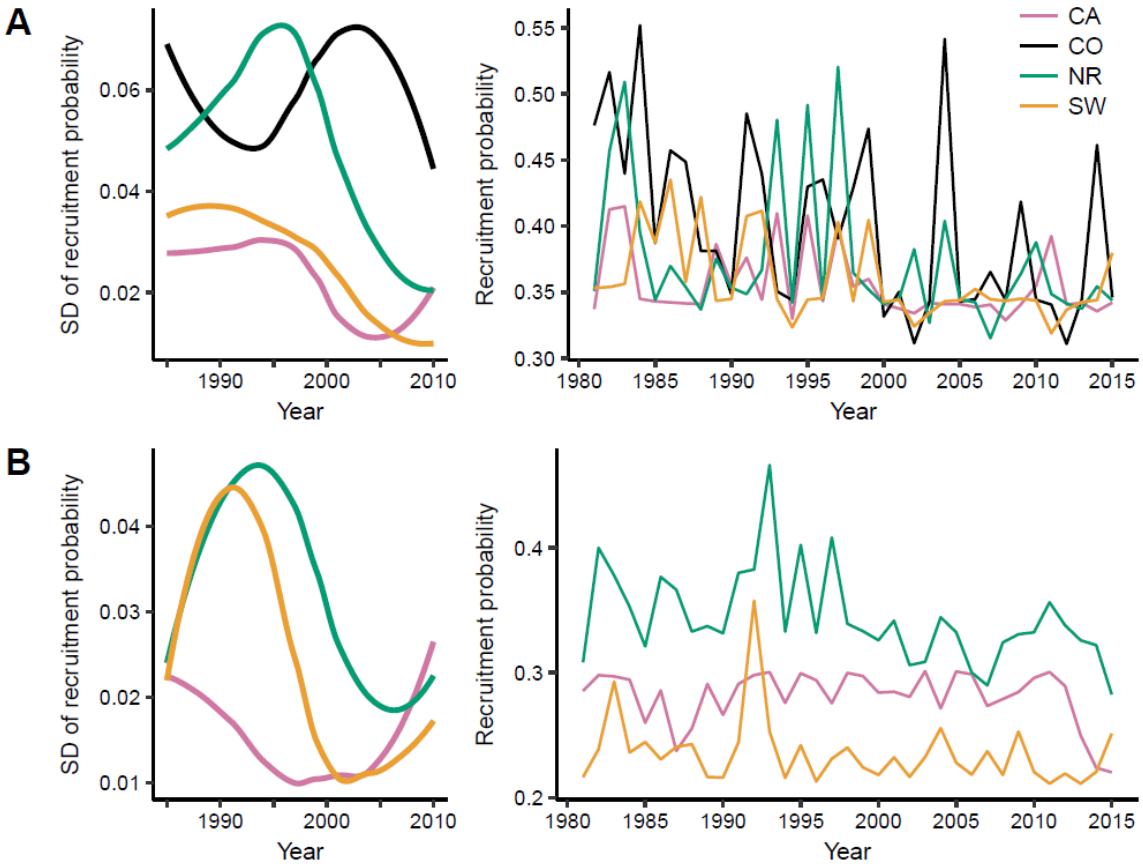

Figure S6. Probability of crossing the region-specific recruitment threshold (recruitment probability) and the variability in recruitment probability over time for ponderosa pine (A) and Douglas-fir (B). For predictions of recruitment probability time since fire (1 yr), distance to seed source (50 m), and fire severity (dNBR 412) were held constant. The standard deviation (SD) of recruitment probability was calculated in moving 10 year windows with the year on the x-axis representing the center of each window and summarized with locally weighted polynomial regression smoothing (LOESS). The recruitment threshold in these models was 4 trees/ha (lowest density recorded in any plot in any year) which is equivalent to modeling the presence or absence of at least one seedling in a plot in each year.

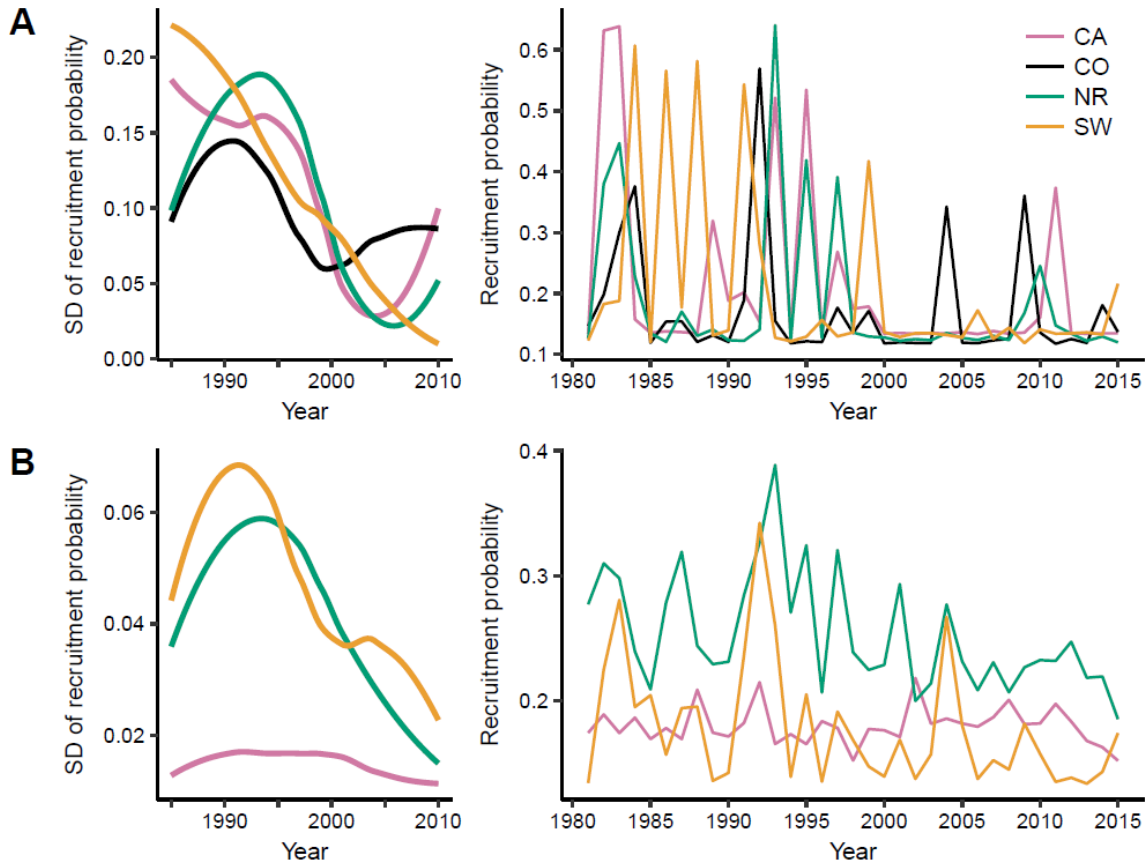

Figure S7. Probability of crossing the region-specific recruitment threshold (recruitment probability) and the variability in recruitment probability over time for ponderosa pine (A) and Douglas-fir (B). For predictions of recruitment probability time since fire (1 yr), distance to seed source (50 m), and fire severity (dNBR 412) were held constant. The standard deviation (SD) of recruitment probability was calculated in moving 10 year windows with the year on the x-axis representing the center of each window and summarized with locally weighted polynomial regression smoothing (LOESS). The recruitment threshold in these models was the 50th percentile of recruitment density for years with recruitment for a given species in a given region (Table S1).

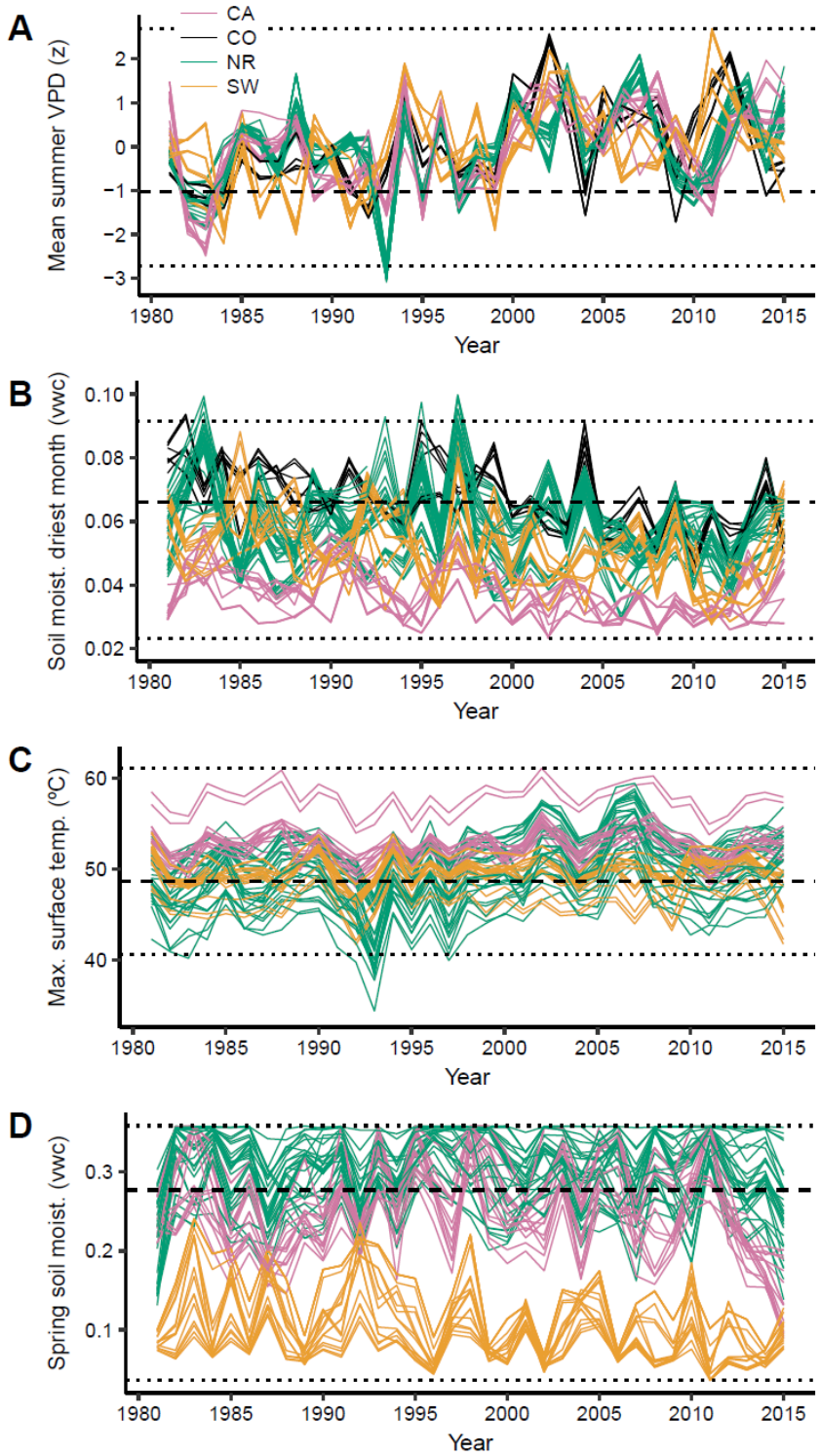

Figure S8. Time series of climate variables at each site (n=90) that were used to predict changes in annual recruitment probability over time (Figs. 3F & 4F). The dashed line represents the threshold value identified by the BRT models (Figs. 3A, 3C, 4A, & 4C) and the dotted lines represent the maximum and the minimum values used to fit the BRT models (i.e. when we use the BRT models to predict to annual climate conditions outside the dotted lines it is extrapolation).

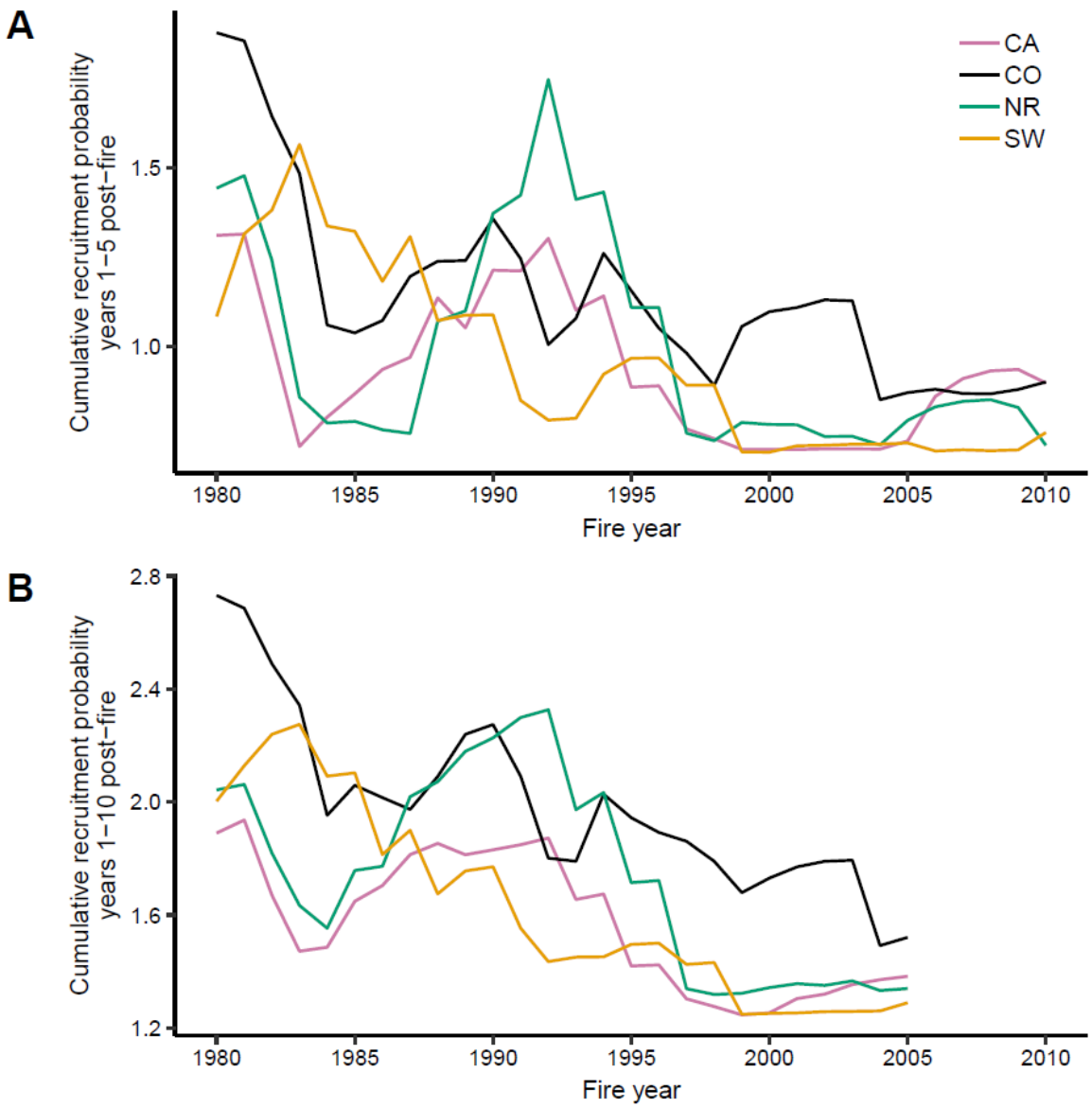

Figure S9. Modeled cumulative recruitment probability for ponderosa pine in the first five (A) or ten (B) years following fire, while holding constant distance to seed source (50 m) and fire severity (dNBR 412). The recruitment threshold in these models was the 25th percentile of recruitment density for years with recruitment for a given species in a given region (model presented in main text; Table S1).

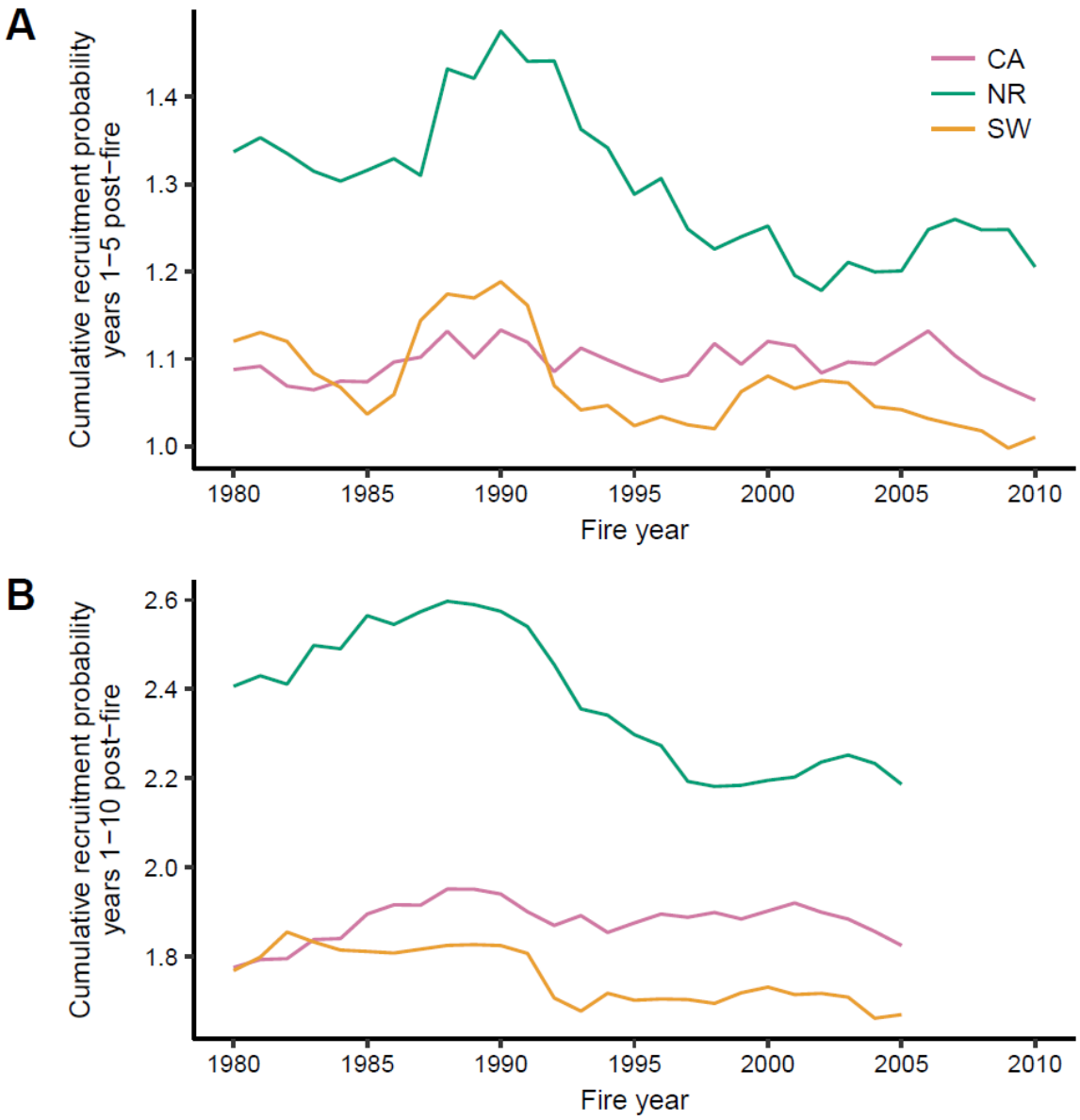

Figure S10. Modeled cumulative recruitment probability for Douglas-fir in the first five (A) or ten (B) years following fire, while holding constant distance to seed source (50 m) and fire severity (dNBR 412). The recruitment threshold in these models was the 25th percentile of recruitment density for years with recruitment for a given species in a given region (model presented in main text; Table S1).

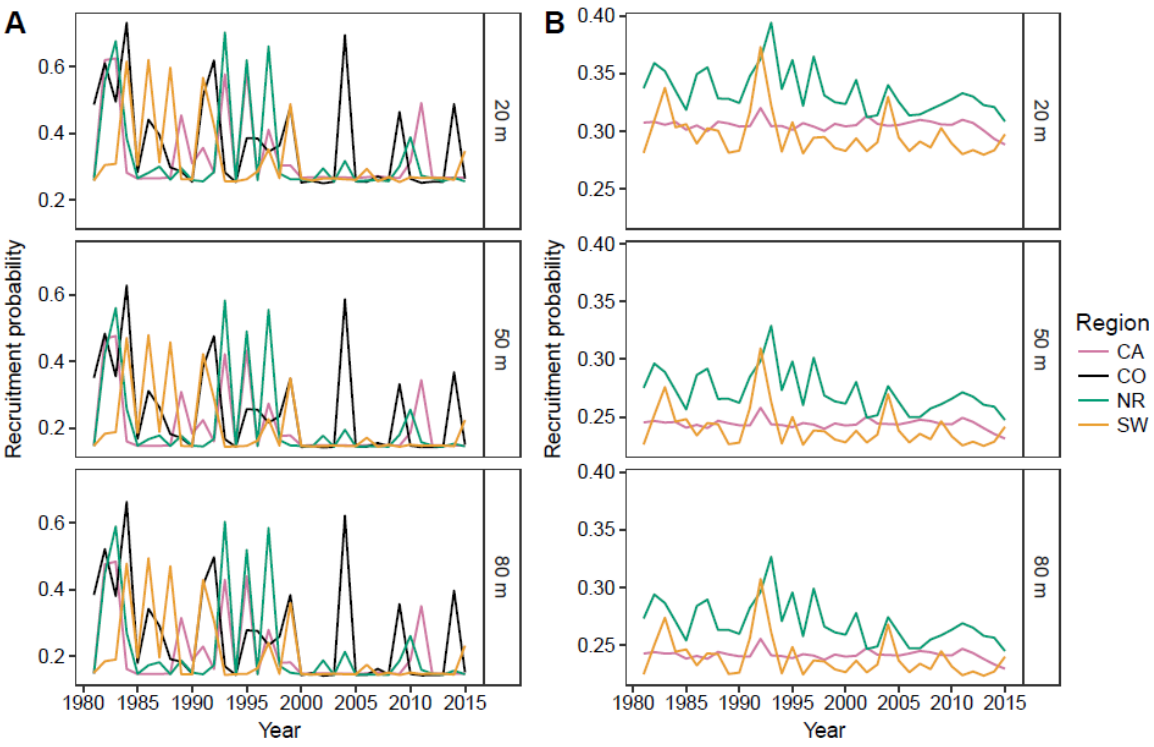

Figure S11. Probability of crossing the region-specific recruitment threshold (recruitment probability) for ponderosa pine (A) and Douglas-fir (B). For predictions of recruitment probability time since fire (1 yr) and fire severity (dNBR 412) were held constant. Distance to seed source was set at 20, 50, or 80 m. The recruitment threshold in these models was the 25th percentile of recruitment density for years with recruitment for a given species in a given region (Table S1).

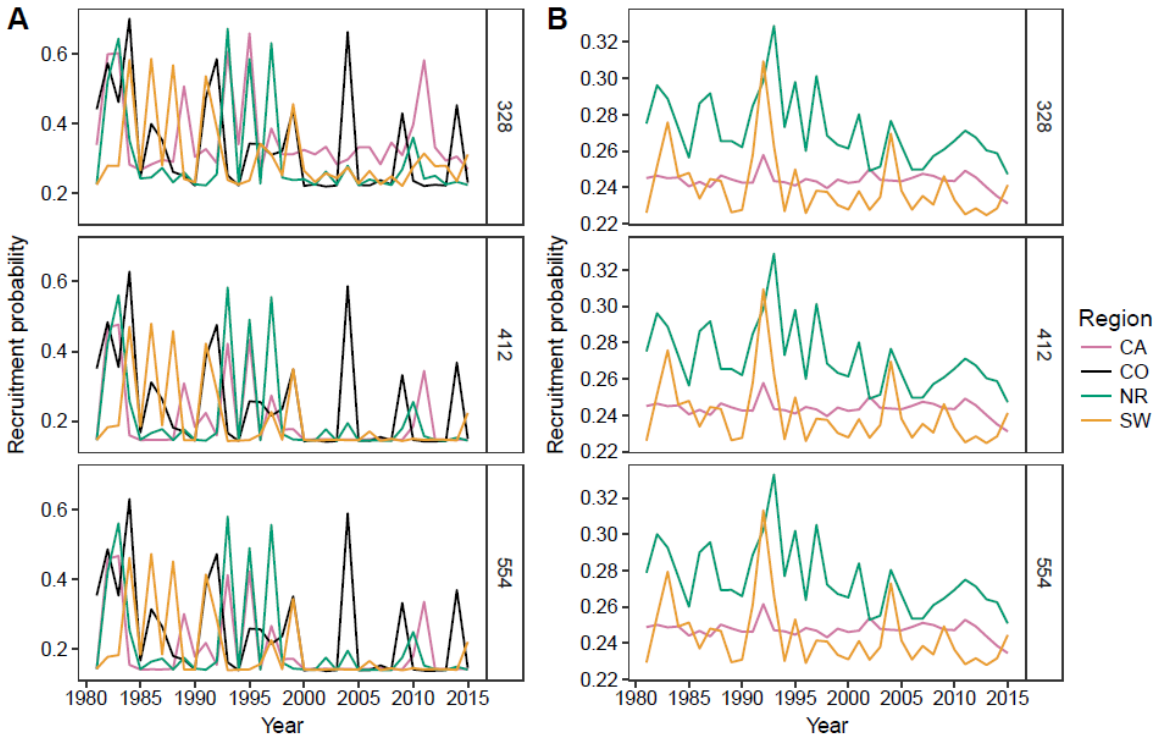

Figure S12. Probability of crossing the region-specific recruitment threshold (recruitment probability) for ponderosa pine (A) and Douglas-fir (B). For predictions of recruitment probability time since fire (1 yr) and distance to seed source (50 m) were held constant. Fire severity was set to the dNBR (differenced normalized burn ratio) value that corresponded to the 25th (328), 50th (412), and 75th (554) percentile of the fire severity experienced at the sample sites. The recruitment threshold in these models was the 25th percentile of recruitment density for years with recruitment for a given species in a given region (Table S1).

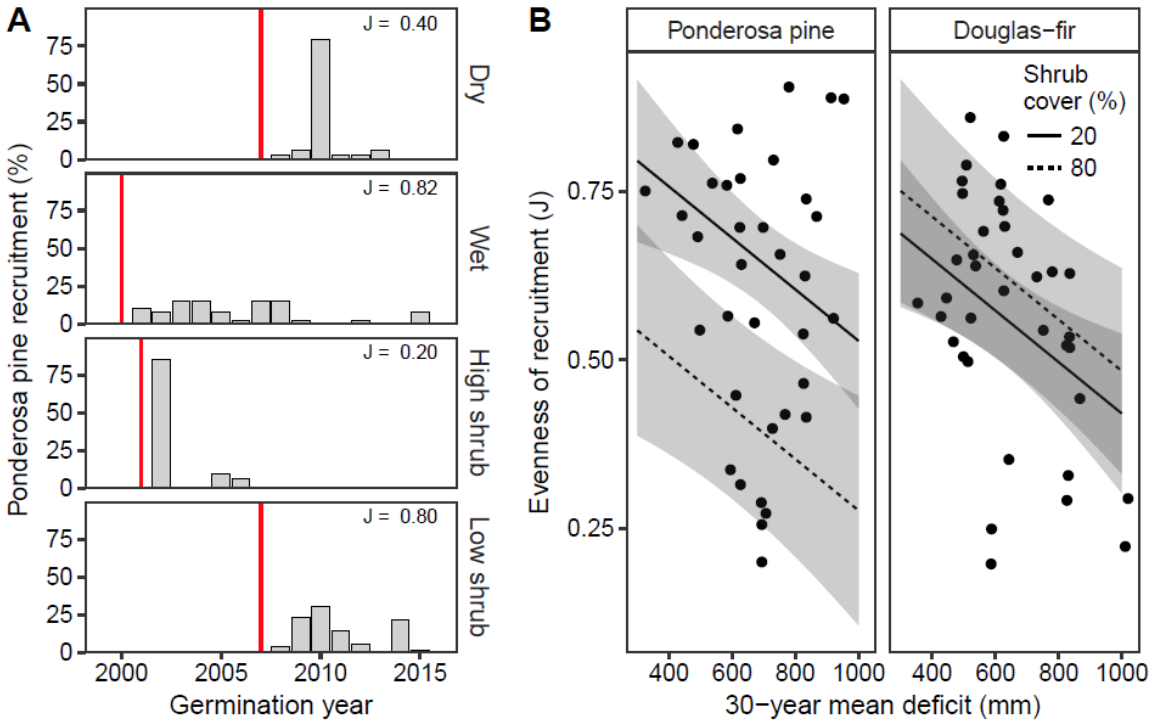

Figure S13. Representative age structures from four ponderosa pine sites (A); each panel represents one site. The top two panels show sites with high (728 mm) and low (428 mm) mean annual water deficit ("Dry" and "Wet", respectively) from the Northern Rockies. The bottom two panels show sites with high (80%) and low (19%) shrub cover from California. Evenness of recruitment scales from 0 (episodic recruitment) to 1 (continuous recruitment). The red vertical line represents the fire year at each site. Age structures for all sites are in Figs. S14-22. Evenness of recruitment (*J*) for all sites in California, Northern Rockies, and the Southwest compared to 30-year mean climatic water deficit (B). Fitted lines for sites with a shrub cover of 20% and 80% are represented by solid and dashed lines respectively. Shaded areas represent 95% confidence intervals. Shrub cover data were not collected in CO and thus CO sites were excluded from this analysis.

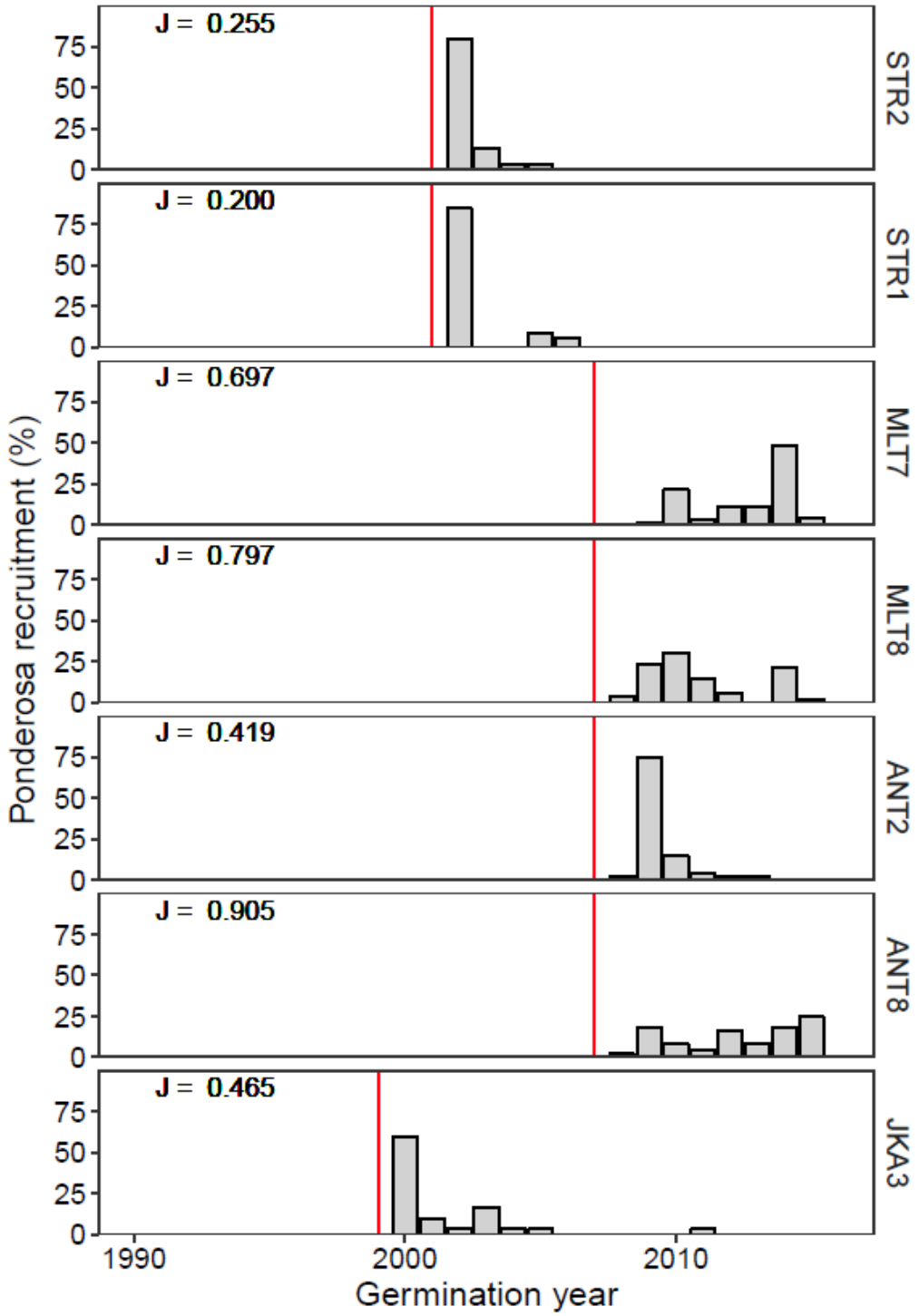

Figure S14. Age structures from California (CA) ponderosa pine (*P. ponderosa*) sites showing the percent of total recruitment at each site that occurred in each year. Each box represents one site. Sites are organized from wettest at the top to driest at the bottom based on 30-year (1980-2009) deficit. "J" is evenness of recruitment over time at each site. The red vertical line represents the fire year.

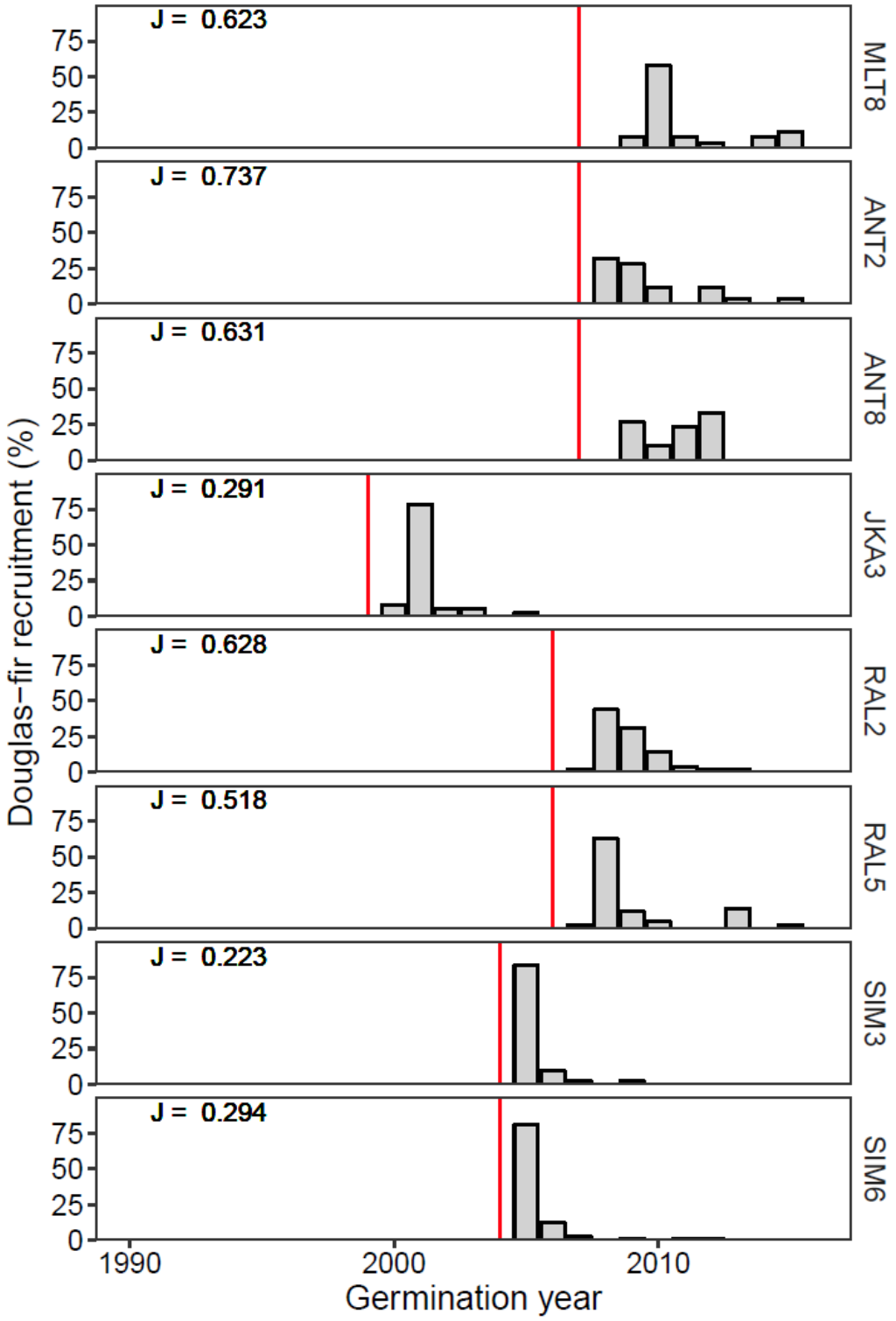

Figure S15. Age structures from California (CA) Douglas-fir (*Pseudotsuga menziesii*) sites showing the percent of total recruitment at each site that occurred in each year. Each box represents one site. Sites are organized from wettest at the top to driest at the bottom based on 30-year (1980-2009) deficit. "J" is evenness of recruitment over time at each site. The red vertical line represents the fire year.

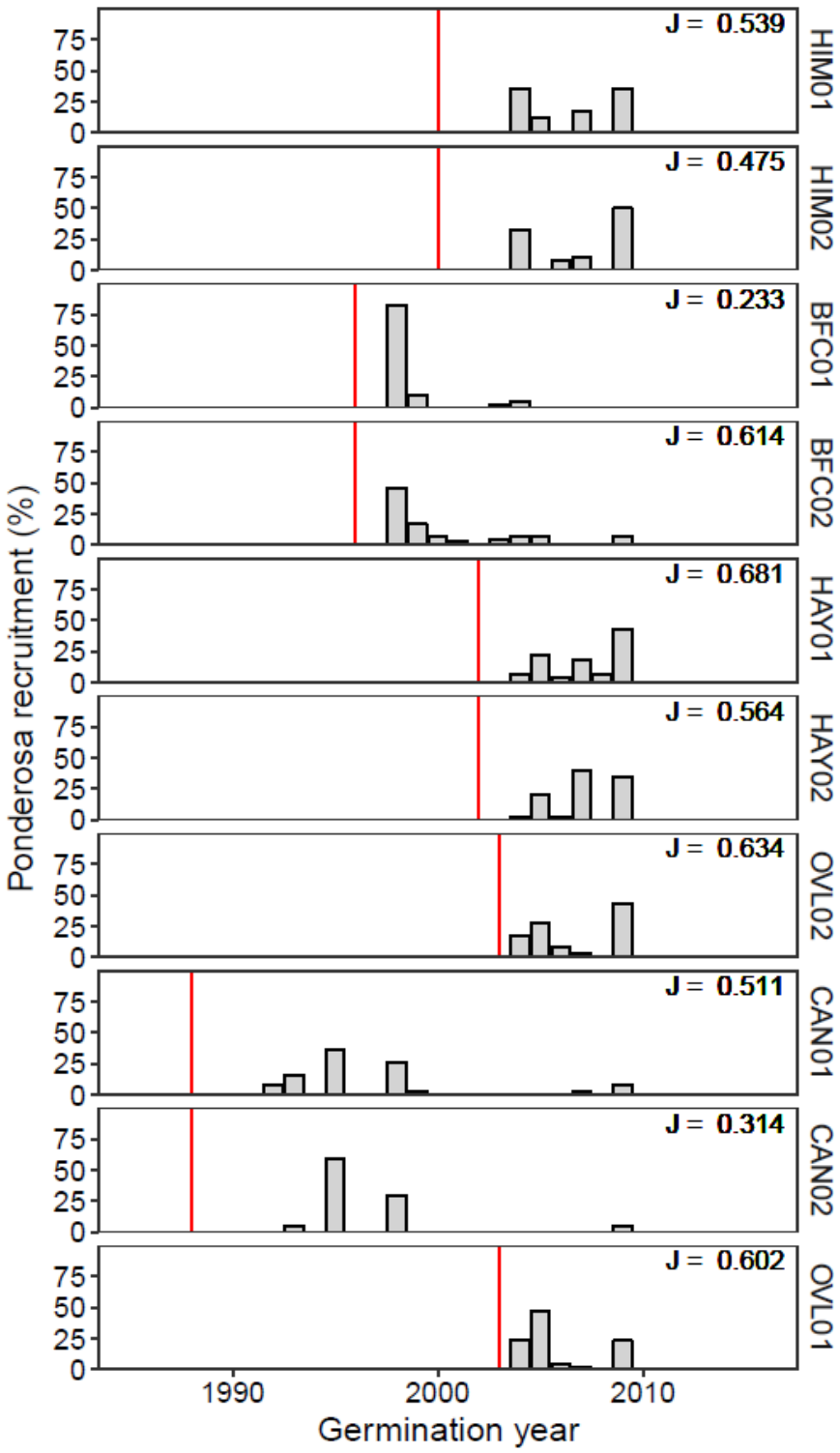

Figure S16. Age structures from Colorado (CO) ponderosa pine (*Pinus ponderosa*) sites showing the percent of total recruitment at each site that occurred in each year. Each box represents one site. Sites are organized from wettest at the top to driest at the bottom based on 30-year (1980-2009) deficit. "J" is evenness of recruitment over time at each site. The red vertical line represents the fire year.

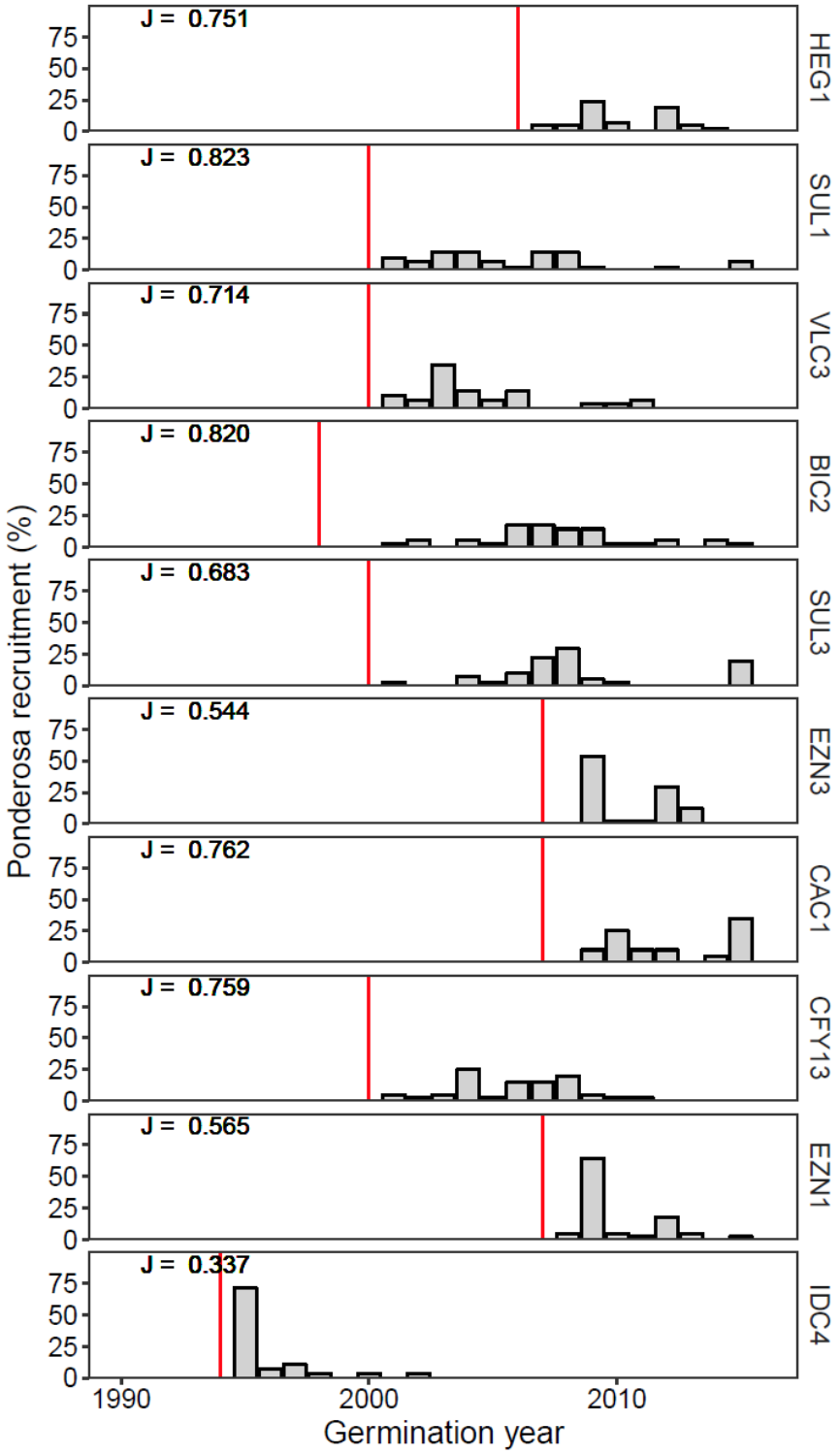

Figure S17. Age structures from the 10 wettest Northern Rockies (NR) ponderosa pine (*Pinus ponderosa*) sites showing the percent of total recruitment at each site that occurred in each year. Each box represents one site. Sites are organized from wettest at the top to driest at the bottom based on 30-year (1980-2009) deficit. "J" is evenness of recruitment over time at each site. The red vertical line represents the fire year.

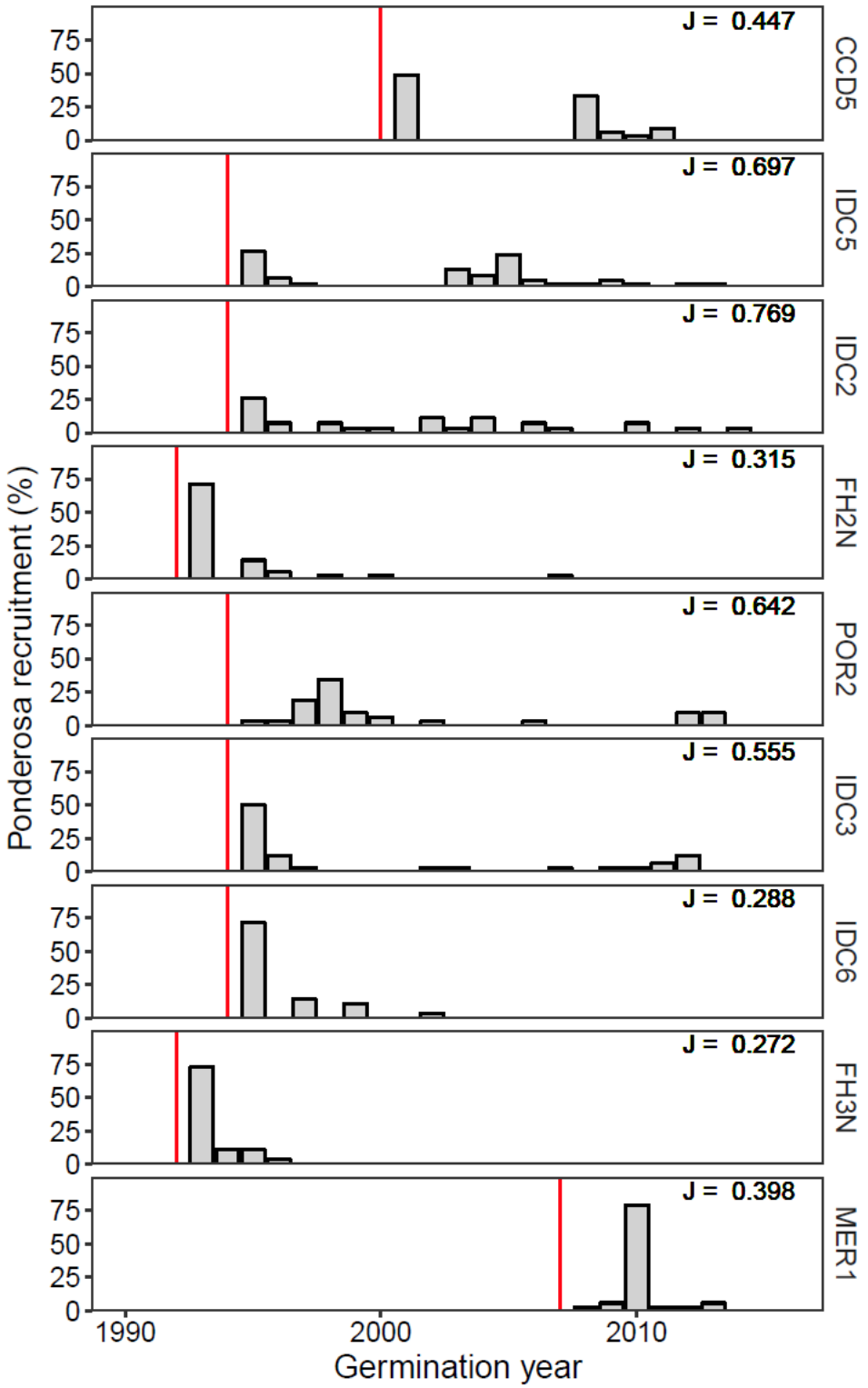

Figure S18. Age structures from the 10 driest Northern Rockies (NR) ponderosa pine (*Pinus ponderosa*) sites showing the percent of total recruitment at each site that occurred in each year. Each box represents one site. Sites are organized from wettest at the top to driest at the bottom based on 30-year (1980-2009) deficit. "J" is evenness of recruitment over time at each site. The red vertical line represents the fire year.

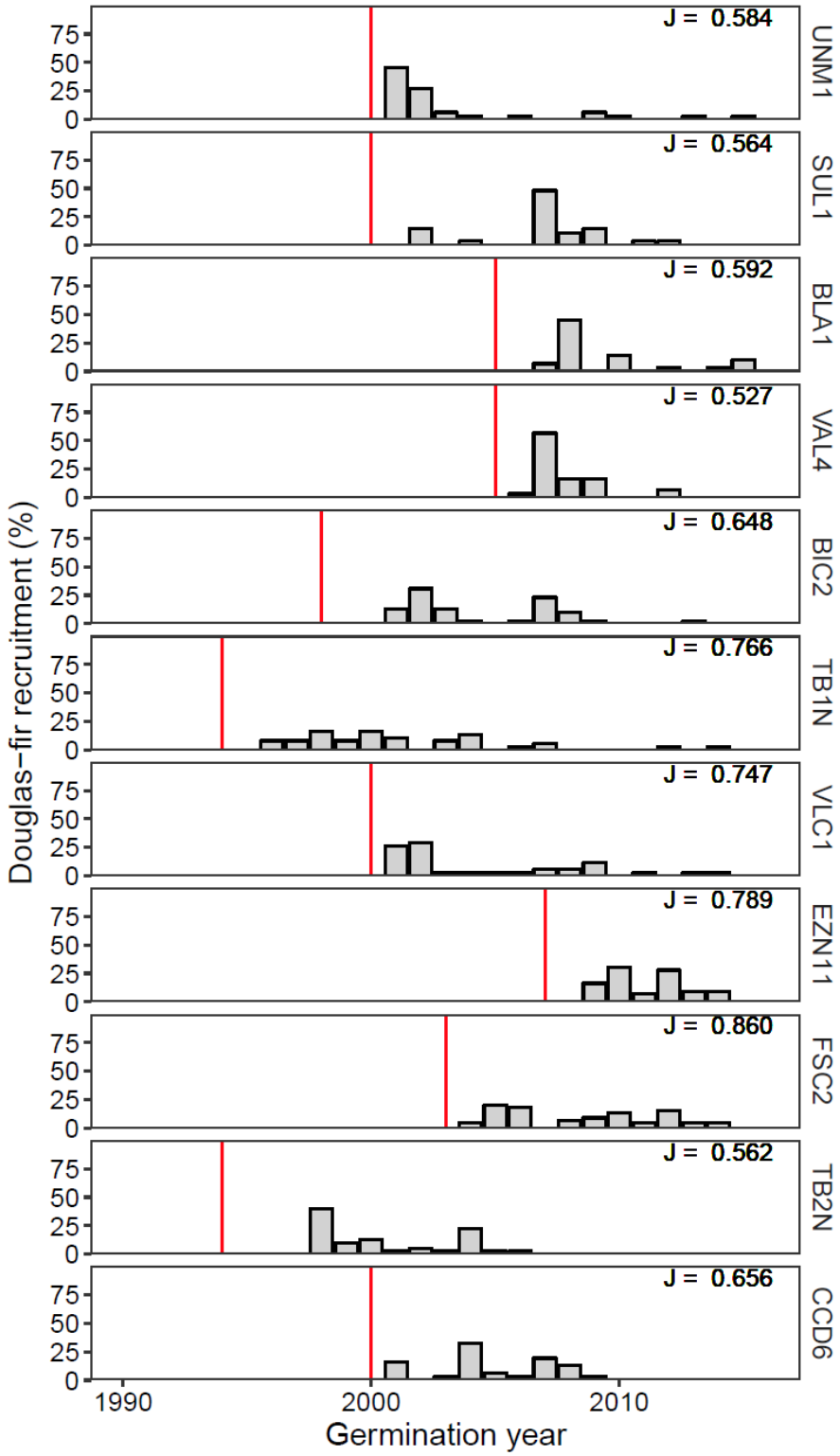

Figure S19. Age structures from the 11 wettest Northern Rockies (NR) Douglas-fir (*Pseudotsuga menziesii*) sites showing the percent of total recruitment at each site that occurred in each year. Each box represents one site. Sites are organized from wettest at the top to driest at the bottom based on 30-year (1980-2009) deficit. "J" is evenness of recruitment over time at each site. The red vertical line represents the fire year.

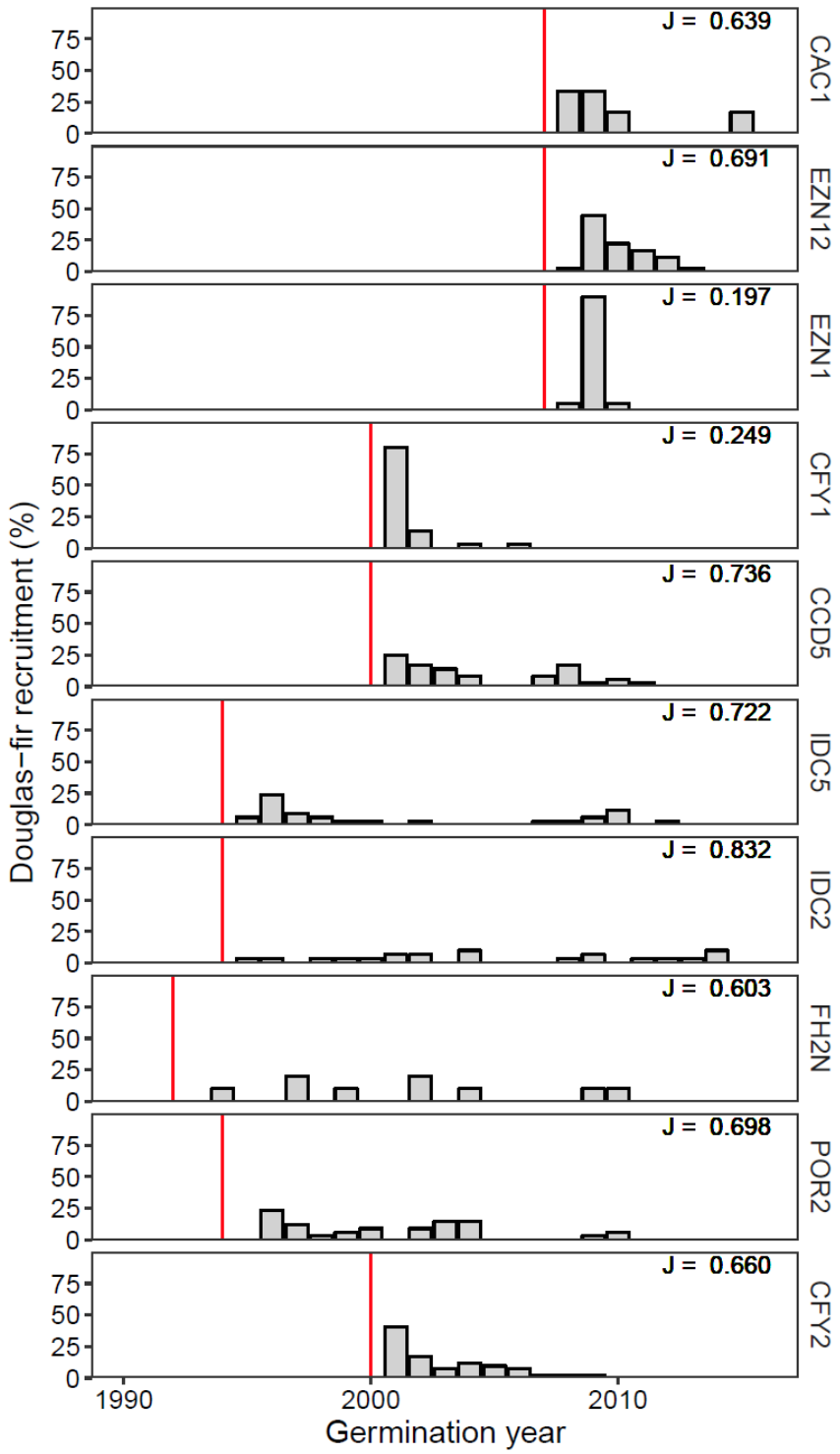

Figure S20. Age structures from the 10 driest Northern Rockies (NR) Douglas-fir (*Pseudotsuga menziesii*) sites showing the percent of total recruitment at each site that occurred in each year. Each box represents one site. Sites are organized from wettest at the top to driest at the bottom based on 30-year (1980-2009) deficit. "J" is evenness of recruitment over time at each site. The red vertical line represents the fire year.

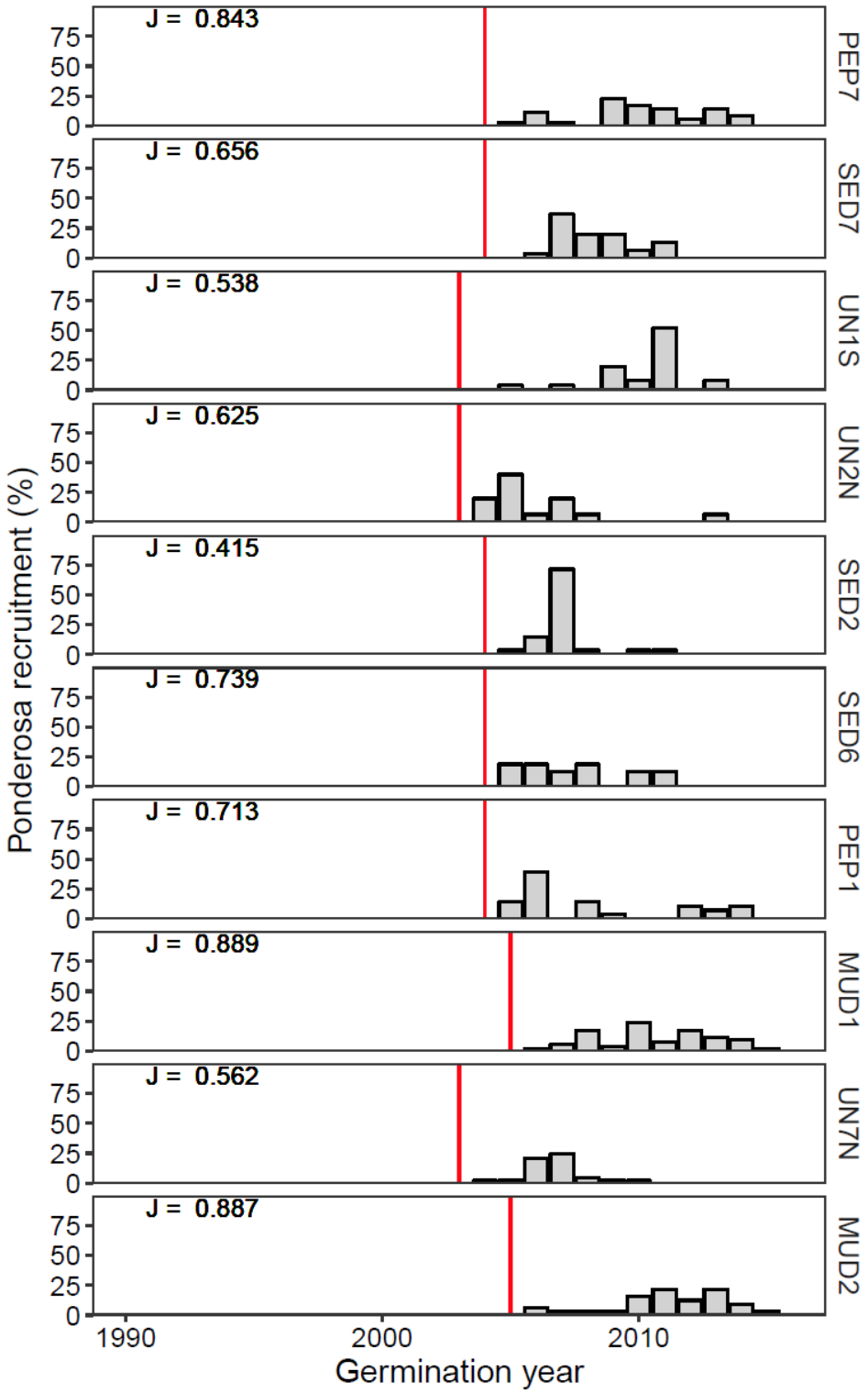

Figure S21. Age structures from the Southwest (SW) ponderosa pine (*Pinus ponderosa*) sites showing the percent of total recruitment at each site that occurred in each year. Each box represents one site. Sites are organized from wettest at the top to driest at the bottom based on 30-year (1980-2009) deficit. "J" is evenness of recruitment over time at each site. The red vertical line represents the fire year.

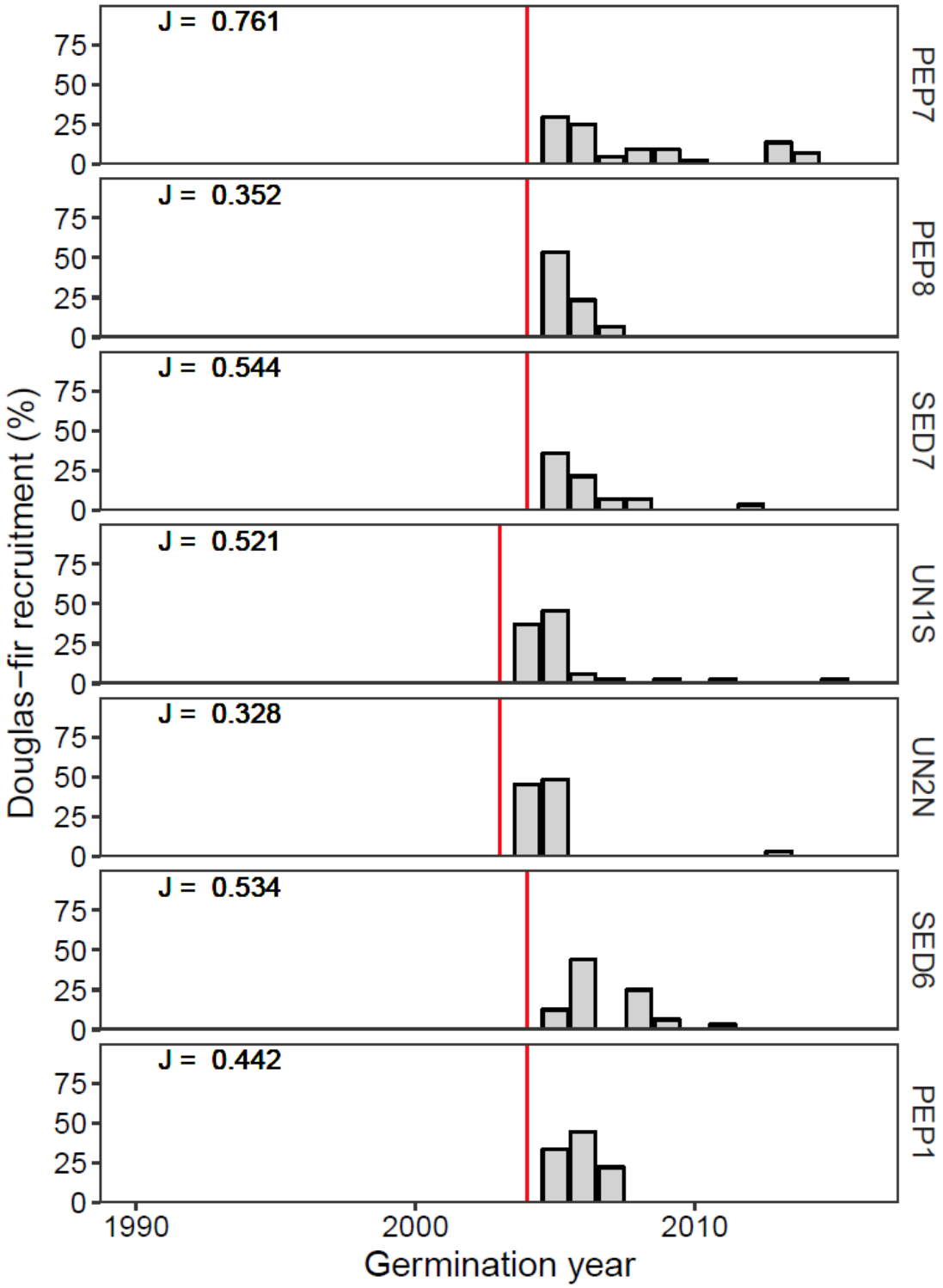

Figure S22. Age structures from the Southwest (SW) Douglas-fir (*Pseudotsuga menziesii*) sites showing the percent of total recruitment at each site that occurred in each year. Each box represents one site. Sites are organized from wettest at the top to driest at the bottom based on 30-year (1980-2009) deficit. "J" is evenness of recruitment over time at each site. The red vertical line represents the fire year.

Table S1. Number of sites and trees sampled in each region, 30-year (1980-2009) mean annual climatic water deficit for those sites, and annual recruitment rate used as a threshold in each region for modeling a binomial response. Thresholds are the 25th or 50th percentile of annual recruitment rate for each species in each region for years in which at least one seedling established. Some sites had both species. PIPO is ponderosa pine and PSME is Douglas-fir.

Region	Species	Sites	Juveniles	Mean annual deficit (mm)	25th percentile threshold (trees ha^{-1} yr^{-1})	50th percentile threshold (trees ha^{-1} yr^{-1})
CA	PIPO	13	320	741	17	53
	PSME	16	320	851	17	42
	total	**19**	**640**	**800**		
CO	PIPO	10	355	603	16	80
	PSME	0	0	-		
	total	**10**	**355**	**603**		
NR	PIPO	32	658	572	42	71
	PSME	29	670	538	56	129
	total	**40**	**1328**	**554**		
SW	PIPO	16	297	835	13	25
	PSME	18	200	768	12	24
	total	**21**	**497**	**807**		
All	PIPO	71	1630	-		
	PSME	63	1190	-		
	total	**90**	**2820**	-		

Table S2. Region, fire name, fire year, species sampled, and coordinates of all sites.

Site	Region	Fire	Fire year	Species	Latitude	Longitude
ANT2	CA	Antelope Complex	2007	both	40.1013	-120.6277
ANT8	CA	Antelope Complex	2007	both	40.1111	-120.6293
ANT1N	CA	Antelope Complex	2007	PSME	40.1110	-120.6289
ANT1S_ADJ	CA	Antelope Complex	2007	PSME	40.1077	-120.6322
ANT2S	CA	Antelope Complex	2007	PSME	40.1020	-120.6275
JKA3	CA	Jackass	1999	both	40.8427	-122.4299
JKA1N	CA	Jackass	1999	PIPO	40.8466	-122.4686
JKA3S_ADJ	CA	Jackass	1999	PSME	40.8400	-122.4318
MLT7	CA	Moonlight	2007	both	40.1842	-120.8150
MLT8	CA	Moonlight	2007	both	40.2089	-120.8212
MLT4N	CA	Moonlight	2007	PIPO	40.2007	-120.8200
MLT4S	CA	Moonlight	2007	PSME	40.2000	-120.8196
RAL2	CA	Ralston	2006	both	39.0284	-120.6957
RAL5	CA	Ralston	2006	both	39.0291	-120.6903
RAL2S	CA	Ralston	2006	PIPO	39.0269	-120.6951
SIM6	CA	Sims	2004	both	40.7121	-123.5354
SIM3	CA	Sims	2004	PSME	40.7168	-123.5424
STR1	CA	Star	2001	both	39.1185	-120.5108
STR2	CA	Star	2001	both	39.1188	-120.5097
BFC01	CO	Buffalo Creek	1996	PIPO	39.3753	-105.2608
BFC02	CO	Buffalo Creek	1996	PIPO	39.3733	-105.2722
Can01	CO	Canyon	1988	PIPO	40.1195	-105.3255
Can02	CO	Canyon	1988	PIPO	40.1188	-105.3256
HAY01	CO	Hayman	2002	PIPO	39.1824	-105.1695
HAY02	CO	Hayman	2002	PIPO	39.1817	-105.1683
HIM01	CO	High Meadows	2000	PIPO	39.4097	-105.3667
HIM02	CO	High Meadows	2000	PIPO	39.4075	-105.3511
OVL01	CO	Overland	2003	PIPO	40.1428	-105.3167
OVL02	CO	Overland	2003	PIPO	40.1353	-105.3228
BIC1	NR	Bitterroot Complex	1998	both	45.9693	-114.0004
BIC2	NR	Bitterroot Complex	1998	both	45.9696	-114.0042
BLA1	NR	Blackerby	2005	PSME	45.8854	-116.0304
CFY1	NR	Canyon Ferry	2000	both	46.6904	-111.7031
CFY1N	NR	Canyon Ferry	2000	both	46.6907	-111.7042
CFY2	NR	Canyon Ferry	2000	both	46.6703	-111.6883
CFY13	NR	Canyon Ferry	2000	PIPO	46.6980	-111.7107
CFY1S	NR	Canyon Ferry	2000	PIPO	46.6929	-111.7072
CFY2S	NR	Canyon Ferry	2000	PIPO	46.6671	-111.6876
CAC1	NR	Cascade Complex	2007	both	44.6778	-115.6571
CCD5	NR	Clear Creek Divide	2000	both	45.3312	-114.2577
CCD6	NR	Clear Creek Divide	2000	PSME	45.1359	-114.2121

Table S2 continued.

Site	Region	Fire	Fire year	Species	Latitude	Longitude
EAR1	NR	Earthquake	2001	PIPO	45.8330	-115.9713
EZN1	NR	East Zone	2007	both	45.0534	-115.7493
EZN11	NR	East Zone	2007	both	45.0817	-115.7633
EZN12	NR	East Zone	2007	both	44.9576	-115.7237
EZN12S	NR	East Zone	2007	both	44.9544	-115.7260
EZN2S	NR	East Zone	2007	both	45.1802	-115.5795
EZN1S	NR	East Zone	2007	PIPO	45.0541	-115.7494
EZN3	NR	East Zone	2007	PIPO	45.2057	-115.5847
FSC2	NR	Fish Creek	2003	PSME	46.9879	-114.6699
FH2N	NR	Foothills	1992	both	43.5572	-115.5510
FH3N	NR	Foothills	1992	PIPO	43.5775	-115.6948
FH2S	NR	Foothills	1992	PSME	43.5585	-115.5563
HEG1	NR	Heaven's Gate	2006	both	45.4582	-116.1210
IDC4	NR	Idaho City Complex	1994	both	43.9315	-115.5215
IDC6	NR	Idaho City Complex	1994	both	43.8261	-115.5528
IDC2	NR	Idaho City Complex	1994	both	43.9569	-115.4657
IDC5	NR	Idaho City Complex	1994	both	43.9450	-115.4468
IDC3	NR	Idaho City Complex	1994	PIPO	43.9025	-115.4514
MER1	NR	Meriwether	2007	PIPO	46.8208	-111.9274
POR2	NR	Porphyry South	1994	both	45.1815	-115.5706
SUL1	NR	Sula Complex	2000	both	45.9037	-114.1695
SUL3	NR	Sula Complex	2000	PIPO	45.9050	-114.1665
TB1N	NR	Thunderbolt	1994	PSME	44.7939	-115.5489
TB2N	NR	Thunderbolt	1994	PSME	44.7925	-115.5426
UNM1	NR	Upper Ninemile	2000	PSME	47.2191	-114.5760
VLC1	NR	Valley Complex	2000	both	45.9719	-114.0224
VLC3	NR	Valley Complex	2000	PIPO	46.0043	-114.0303
VAL4	NR	Valley Road	2005	PSME	44.0414	-114.7574
MUD1	SW	Mudersbach	2005	PIPO	35.8708	-111.9316
MUD2	SW	Mudersbach	2005	PIPO	35.8561	-111.9092
PEP1	SW	Peppin	2004	both	33.6192	-105.4752
PEP2bN	SW	Peppin	2004	both	33.6367	-105.5082
PEP3S	SW	Peppin	2004	both	33.6256	-105.4669
PEP5N	SW	Peppin	2004	both	33.6146	-105.4759
PEP7	SW	Peppin	2004	both	33.6130	-105.4413
PEP8	SW	Peppin	2004	both	33.6150	-105.4494
PEP2S_ADJ	SW	Peppin	2004	PIPO	33.6335	-105.5161
PEP5S	SW	Peppin	2004	PSME	33.6197	-105.4763
SED2	SW	Sedgewick	2004	both	35.1987	-108.1008
SED6	SW	Sedgewick	2004	both	35.1985	-108.1011

Table S2 continued.

Site	Region	Fire	Fire year	Species	Latitude	Longitude
SED6S	SW	Sedgewick	2004	both	35.1991	-108.1014
SED7	SW	Sedgewick	2004	both	35.1725	-108.0896
SED2S	SW	Sedgewick	2004	PSME	35.1991	-108.1008
SED3N	SW	Sedgewick	2004	PSME	35.1764	-108.0816
SED3S	SW	Sedgewick	2004	PSME	35.1714	-108.0827
UN1S	SW	Unnamed	2003	both	33.3603	-107.8339
UN2N	SW	Unnamed	2003	both	33.3592	-107.8283
UN7N	SW	Unnamed	2003	both	33.4012	-107.7994
UN6N	SW	Unnamed	2003	PSME	33.4014	-107.7997

Table S3. Correlation between annual climate variables used in the final BRT models. The ponderosa pine model included mean summer vapor pressure deficit (VPD) and mean soil moisture of the driest month as predictors. The Douglas-fir model included maximum (max) surface temperature and mean spring (March – May) soil moisture.

Species	Variable 1	Variable 2	Correlation
Ponderosa pine	Summer VPD	Soil moisture driest month	-0.26
Ponderosa pine	Summer VPD	Max surface temperature	0.31
Ponderosa pine	Summer VPD	Spring soil moisture	-0.13
Ponderosa pine	Soil moisture driest month	Max surface temperature	-0.38
Ponderosa pine	Soil moisture driest month	Spring soil moisture	0.02
Ponderosa pine	Max surface temperature	Spring soil moisture	0.26
Douglas-fir	Summer VPD	Soil moisture driest month	-0.22
Douglas-fir	Summer VPD	Max surface temperature	0.30
Douglas-fir	Summer VPD	Spring soil moisture	-0.12
Douglas-fir	Soil moisture driest month	Max surface temperature	-0.45
Douglas-fir	Soil moisture driest month	Spring soil moisture	0.17
Douglas-fir	Max surface temperature	Spring soil moisture	0.07

Table S4. Mean accuracy (proportion of years with correct prediction), AUC, and H measure (coherent AUC alternative; ref. 9) by region from spatially independent cross-validation by site for the ponderosa pine (PIPO) and Douglas-fir (PSME) BRT models. When calculating accuracy, the threshold for determining success or failure of recruitment from the modeled probabilities was the value that maximized specificity and sensitivity for each site (Youden's J statistic; ref. 6). Based on ANOVA and post-hoc Tukey's tests, accuracy, AUC, and H measure were not statistically different between regions (P>0.05). Sites that had all 0's or all 1's could not be included in AUC statistics. For PIPO this was 24 of 71 sites and for PSME this was 27 of 63 sites. These sites had a mean accuracy of 0.70 and 0.65 (PIPO and PSME respectively).

		CA	CO	NR	SW
PIPO	Accuracy	0.77	0.79	0.70	0.66
	AUC	0.79	0.79	0.79	0.78
	H measure	0.57	0.55	0.57	0.61
PSME	Accuracy	0.75	NA	0.73	0.85
	AUC	0.89	NA	0.77	0.90
	H measure	0.78	NA	0.53	0.79

Table S5. Transition years in modeled recruitment probability timeseries as identified by a change-point detection algorithm (sup(F) tests). Time series included annual recruitment probability in the first year following fire (1 yr post-fire), and cumulative recruitment probability in the first five or 10 years following fire (5 or 10 yr post-fire, respectively). All transitions were associated with a decline in recruitment probability in the more recent time period except for PSME 10 yr post-fire in CA where recruitment probability increased following 1984. PIPO is ponderosa pine and PSME is Douglas-fir.

	CA		CO		NR		SW	
	shift	*P*	shift	*P*	shift	*P*	shift	*P*
PIPO 1 yr post-fire	NA	0.157	1985	0.046	NA	0.108	1991	0.009
PIPO 5 yr post-fire	1994	<0.001	1983	<0.001	1996	<0.001	1990	<0.001
PIPO 10 yr post-fire	1994	<0.001	1983	<0.001	1996	<0.001	1990	<0.001
PSME 1 yr post-fire	NA	0.550	NA	NA	1996	<0.001	NA	0.088
PSME 5 yr post-fire	NA	0.088	NA	NA	1996	<0.001	1991	<0.001
PSME 10 yr post-fire	1984	<0.001	NA	NA	1992	<0.001	1991	<0.001

References

1. Rother MT, Veblen TT (2017) Climate Drives Episodic Conifer Establishment after Fire in Dry Ponderosa Pine Forests of the Colorado Front Range, USA. Forests 8(5): 159.
2. Holden ZA, et al. (2018) Decreasing fire season precipitation increased recent western US forest wildfire activity. Proc Natl Acad Sci USA 115(36):E8349-E8357.
3. Maneta MP, Silverman NL (2013) A Spatially Distributed Model to Simulate Water, Energy, and Vegetation Dynamics Using Information from Regional Climate Models. Earth Interactions 17(11):1-44.
4. Simeone C, et al. (2018) Coupled ecohydrology and plant hydraulics modeling predicts ponderosa pine seedling mortality and lower treeline in the U.S. Northern Rocky Mountains. New Phytol. doi: 10.1111/nph.15499. Published online 27 September 2018.
5. Hoylman Z, Jencso K, Hu J, Holden ZA, Martin J (2018) Hydrology across the critical zone: Topography and climate controls on spatial and temporal organization of vapor pressure deficits, soil moisture and shallow subsurface flow. Water Resources Research In Press.
6. Youden WJ (1950) Index for rating diagnostic tests. *Cancer* 3(1):32-35.
7. Dobrowski SZ, *et al.* (2013) The climate velocity of the contiguous United States during the 20th century. *Glob Chang Biol* 19(1):241-251.
8. Mason SJ, Graham NE (2002) Areas beneath the relative operating characteristics (ROC) and relative operating levels (ROL) curves: Statistical significance and interpretation. *Quarterly Journal of the Royal Meteorological Society* 128(584):2145-2166.
9. Hand DJ (2009) Measuring classifier performance: a coherent alternative to the area under the ROC curve. *Machine Learning* 77(1):103-123.